Simple method to characterize nonlinear refraction and loss in optical waveguides

Jeremiah J. Wathen,[1,2,*] Vincent R. Pagán,[1,3] and Thomas E. Murphy[1,3,4]

[1]*Laboratory for Physical Sciences, College Park, Maryland 20740, USA*

[2]*Department of Physics, University of Maryland, College Park, Maryland 20742, USA*

[3]*Department of Electrical & Computer Engineering, University of Maryland, College Park, Maryland 20742, USA*

[4]*Institute for Research in Electronics & Applied Physics, University of Maryland, College Park, Maryland 20742, USA*

**Corresponding author: wathenjj@lps.umd.edu*

Received August 17, 2012; revised October 4, 2012; accepted October 8, 2012;
posted October 8, 2012 (Doc. ID 174504); published November 9, 2012

We describe a technique for accurately measuring the ratio between the imaginary and real parts of the third-order nonlinearity in optical waveguides. Unlike most other methods, it does not depend on precise knowledge of the coupling efficiencies, optical propagation loss, or optical pulse shape. We apply the method to characterize a silicon waveguide, a GaAs waveguide, and AlGaAs waveguides with different alloy concentrations.

OCIS codes: 190.0190, 190.3270, 190.4180, 190.4390, 190.4400, 190.5970.

Low-loss submicrometer waveguides are promising candidates for nonlinear optical signal processing, and could enable chip-scale devices for wavelength conversion, optical switching, and other processes [1]. Nonlinear absorption, which is described by the imaginary part of the nonlinear susceptibility, is recognized as a factor that limits the efficiency of many nonlinear mixing processes [2]. When assessing the suitability of a material or waveguide for nonlinear optics, an important figure of merit is the ratio of the imaginary to the real part of the effective third-order nonlinear susceptibility [3], which we call the nonlinear loss-tangent of a waveguide.

A variety of methods are used to characterize the nonlinear properties of waveguides, including power-dependent spectral broadening [4–6], nonlinear absorption [7,8], four-wave mixing [9–11], and coherent pump-probe measurements [12]. Most methods are hampered by uncertainty associated with poor knowledge of the optical pulse shape, waveguide loss, or input coupling efficiency. We present here a simple and accurate continuous-wave (CW) technique to measure the nonlinear loss tangent that is insensitive to the optical power coupled into the waveguide and the linear loss. We apply the method to characterize the nonlinear loss tangent of optical waveguides made from Si, GaAs, and AlGaAs alloys.

Figure 1 depicts the experiment used to characterize the nonlinear loss tangent. A sinusoidally modulated pump is combined with a weaker CW probe signal, and launched into the waveguide using an aspheric lens. The sinusoidal modulation is imparted onto the probe signal through a combination of cross-phase modulation (XPM) and cross-amplitude modulation (XAM). Following the waveguide, the pump is suppressed by a spectral filter while the probe passes through a 50 km span of dispersive fiber, which converts intensity modulation to phase modulation and vice versa in a frequency-dependent manner [13]. The modulation frequency is then swept while recording the amplitude of the received sinusoidal signal using a network analyzer. This method was originally developed to quantify the chirp of optoelectronic modulators [14], whereas here the modulation is applied through a third-order nonlinear interaction.

We assume that the pump entering the waveguide is sinusoidally modulated, according to

$$P_1(t) = P_{10} + \Delta P \sin \Omega t, \tag{1}$$

where P_{10} is the average pump power, ΔP is the modulation amplitude, and Ω is the modulation frequency. After undergoing XPM and XAM, the probe signal that emerges from the waveguide is described by the field [15]

$$A_2(t) = \sqrt{P_{20}} e^{-i\omega_0 t} \exp[i2\gamma l_{\text{eff}} \Delta P \sin \Omega t], \tag{2}$$

where ω_0 represents the optical frequency, $l_{\text{eff}} \equiv (1 - e^{-\alpha l})/\alpha$ is the effective waveguide length, and the complex coefficient $\gamma \equiv \gamma_R + i\gamma_I$ describes the combined effects of XPM and XAM. If the optical mode is mostly confined to a homogeneous core region, the nonlinear coefficient γ can be expressed as

$$\gamma = \gamma_R + i\gamma_I = \frac{1}{A_{\text{eff}}}\left(\frac{2\pi n_2}{\lambda} + i\frac{\alpha_2}{2}\right), \tag{3}$$

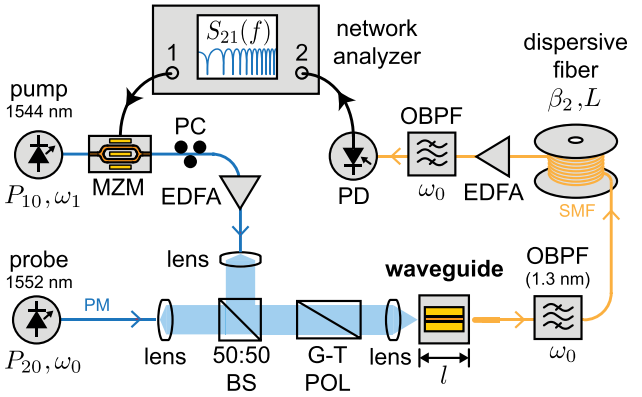

Fig. 1. (Color online) System used to measure the nonlinear loss tangent. MZM, Mach–Zehnder modulator; PC, polarization controller; EDFA, erbium-doped fiber amplifier; BS, beam splitter; G-T POL, Glan–Thompson polarizer; OBPF, optical bandpass filter; PD, photodiode.

where n_2 and α_2 are, respectively, the nonlinear refractive index and two-photon absorption coefficient of the core region, and A_{eff} is the effective area of the optical mode. Equation (3) can be modified to account for the tensor characteristic of the nonlinear susceptibility, polarization states, and overlap between the material and mode [16].

Equation (2) can be Fourier-expanded into a superposition of discrete spectral components,

$$A_2(t) = \sqrt{P_{20}} e^{-i\omega_0 t} \sum_{m=-\infty}^{\infty} J_m(z) e^{im\Omega t}, \tag{4}$$

where we have introduced the complex factor z,

$$z \equiv 2(\gamma_R + i\gamma_I) l_{\text{eff}} \Delta P. \tag{5}$$

In the fiber of length L, each spectral component ω of the signal acquires a phase shift of $\beta(\omega)L$, where the dispersion relation of the fiber is modeled by

$$\beta(\omega) = \beta_0 + \beta_1(\omega - \omega_0) + \frac{\beta_2}{2}(\omega - \omega_0)^2. \tag{6}$$

The signal emerging from the fiber is calculated to be

$$A_2'(t) = \sqrt{P_{20}} e^{-i(\omega_0 t - \beta_0 L)} \sum_{m=-\infty}^{\infty} J_m(z) e^{im\Omega\tau} e^{im^2\beta_2\Omega^2 L/2}, \tag{7}$$

where $\tau \equiv t - \beta_1 L$ denotes the retarded time.

At the receiver, the square-law photodetector with responsivity $\mathcal{R}$ produces a photocurrent of

$$\begin{aligned} i(t) &= \mathcal{R}|A_2'(t)|^2 \\ &= \mathcal{R}P_{20} \sum_m \sum_n \left[J_m(z) J_n(z) \times e^{i(n-m)\Omega\tau} e^{i(n^2-m^2)\beta_2\Omega^2 L/2} \right]. \end{aligned} \tag{8}$$

By expanding Eq. (8) to first order in z, and ignoring the DC term, the photocurrent simplifies to

$$i(t) = -2\mathcal{R}P_{20}|z| \sin(\beta_2\Omega^2 L/2 + \phi) \sin \Omega\tau, \tag{9}$$

or equivalently, in terms of the fiber dispersion D and the cyclic frequency f,

$$i(t) = 2\mathcal{R}P_{20}|z| \sin\left(\frac{\pi\lambda^2 DLf^2}{c} - \phi\right) \sin(2\pi f\tau), \tag{10}$$

where $|z|$ and ϕ represent the magnitude and phase of the complex coefficient z. The phase ϕ is directly related to the nonlinear loss tangent of the waveguide through

$$\tan\phi = \frac{\gamma_I}{\gamma_R} = \frac{\lambda\alpha_2}{4\pi n_2}. \tag{11}$$

Figure 2 shows the measured photocurrent amplitude as a function of frequency for the four different waveguides considered here. The waveguide dimensions, compositions, and calculated mode shapes for the four waveguides are also indicated, to scale, in the upper portion of Fig. 2.

At certain modulation frequencies, the amplitude of the received signal will vanish, leading to a null in the measured $S_{21}(f)$ trace, indicated by the symbols in Fig. 2. From Eq. (10), the null frequencies are given by

$$f_u^2 = \frac{c}{2DL\lambda^2}\left(2u + \frac{2}{\pi}\phi\right), \quad u = 0, 1, 2\ldots \tag{12}$$

Thus, by plotting f_u^2 versus $2u$, we obtain a line whose intercept is related to the phase ϕ. Figure 3 plots f_u^2 versus $2u$ for the silicon waveguide (II), clearly showing this linear behavior. The inset to Fig. 3 plots an enlarged region near the origin, in which we have added the best-fit lines for all four of the waveguides considered. The key in Fig. 3 tabulates the value of the nonlinear loss tangent, $\tan\phi = \gamma_I/\gamma_R$, determined for each of the waveguides.

Among the waveguides considered, the GaAs waveguide exhibits the highest nonlinear loss tangent of $\gamma_I/\gamma_R = 1.12 \pm 0.02$, followed by the silicon waveguide, which gives 0.27 ± 0.02. The remaining two waveguides were composed of $Al_xGa_{1-x}As$ alloys, where the bandgap increases with mole fraction x. For $x = 0.14$, we obtained a lower nonlinear loss tangent of 0.188 ± 0.007. $x \times = 0.18$ when the aluminum fraction is increased to $X = 0.18$ we measure $\gamma_I/\gamma_R = 0.006 \pm 0.002$, indicating that the nonlinearity becomes almost entirely refractive, as

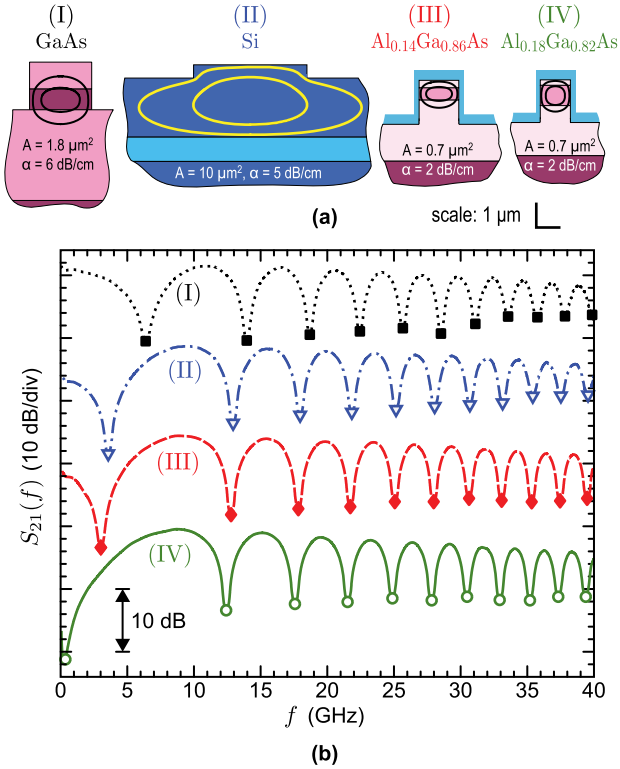

Fig. 2. (Color online) (a) Cross sections and mode properties of the four waveguides studied for this Letter. The contours indicate the −5 and −15 dB levels of the electric field for the TE eigenstate. (b) Representative $S_{21}(f)$ measurement for each waveguide (each offset for clarity).

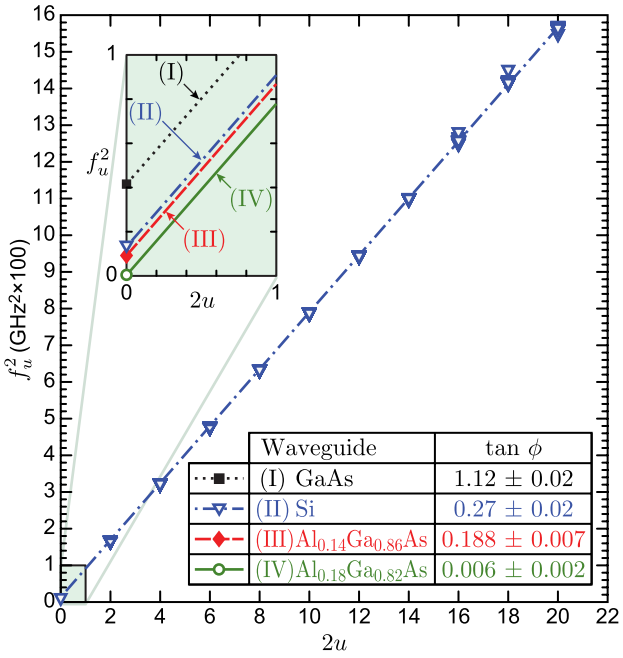

Fig. 3. (Color online) f_u^2 versus $2u$ for the silicon waveguide (II) obtained from 30 consecutive $S_{21}(f)$ measurements. Inset: similar linear fits for all four waveguides considered, enlarged to show difference in intercept.

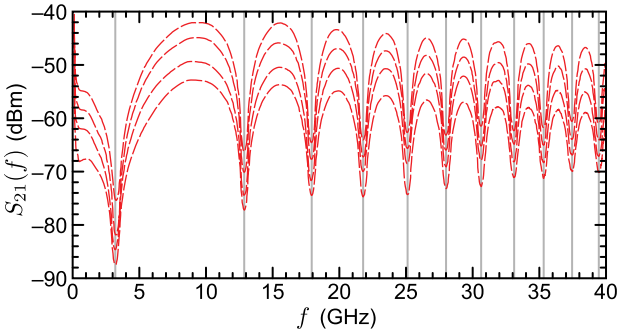

Fig. 4. (Color online) $S_{21}(f)$ measurements from the $Al_{0.14}Ga_{0.86}As$ waveguide, obtained by increasing the pump power in 3 dB steps.

expected when the bandgap exceeds twice the photon energy [17].

For the silicon waveguide (II), the optical mode is almost entirely contained within the silicon ridge, and we therefore expect our results to closely match those of bulk silicon. We conducted independent Z-scan measurements of n_2 and α_2 for crystalline silicon with light polarized along the ⟨110⟩ direction, and found $\tan\phi = \lambda\alpha_2/4\pi n_2 = 0.27 \pm 0.03$, in perfect agreement with the waveguide measurements reported here, and consistent with widely accepted values from the literature [18].

One advantage of this measurement is that it does not require knowledge of the coupling efficiency into the waveguide, a key source of uncertainty in most nonlinear measurements. To illustrate this, Fig. 4 plots four independently measured $S_{21}(f)$ traces obtained by successively increasing the pump power in 3 dB increments. As predicted, the measured result scales, but the positions of the nulls remain unchanged.

In conclusion, we report a new method for measuring the nonlinear loss tangent of optical waveguides. The technique uses a swept-frequency XPM and XAM measurement to circumvent the uncertainties associated with incomplete or inaccurate knowledge of the pulse shape, waveguide loss, and coupling efficiency. When coupled with existing techniques, the method could allow for greater accuracy in completely determining the complex nonlinear coefficients of waveguides.

References

1. M. A. Foster, A. C. Turner, M. Lipson, and A. L. Gaeta, Opt. Express **16**, 1300 (2008).
2. J. S. Aitchison, M. K. Oliver, E. Kapon, E. Colas, and P. W. E. Smith, Appl. Phys. Lett. **56**, 1305 (1990).
3. K. W. DeLong, K. B. Rochford, and G. I. Stegeman, Appl. Phys. Lett. **55**, 1823 (1989).
4. M. Asobe, K. Suzuki, T. Kanamori, and K. Kubodera, Appl. Phys. Lett. **60**, 1153 (1992).
5. C.-Y. Tai, J. Wilkinson, N. Perney, M. Netti, F. Cattaneo, C. Finlayson, and J. Baumberg, Opt. Express **12**, 5110 (2004).
6. Y. Ruan, B. Luther-Davies, W. Li, A. Rode, V. Kolev, and S. Madden, Opt. Lett. **30**, 2605 (2005).
7. A. Villeneuve, C. Yang, G. Stegeman, C. Ironside, G. Scelsi, and R. Osgood, IEEE J. Quantum Electron. **30**, 1172 (1994).
8. T.-K. Liang and H.-K. Tsang, IEEE J. Sel. Top. Quantum Electron. **10**, 1149 (2004).
9. H. Q. Le, W. D. Goodhue, and K. Rauschenbach, Opt. Lett. **15**, 1126 (1990).
10. L. Prigent and J.-P. Hamaide, IEEE Photon. Technol. Lett. **5**, 1092 (1993).
11. H. Fukuda, K. Yamada, T. Shoji, M. Takahashi, T. Tsuchizawa, T. Watanabe, J. Takahashi, and S. Itabashi, Opt. Express **13**, 4629 (2005).
12. Y. Shoji, T. Ogasawara, T. Kamei, Y. Sakakibara, S. Suda, K. Kintaka, H. Kawashima, M. Okano, T. Hasama, H. Ishikawa, and M. Mori, Opt. Express **18**, 5668 (2010).
13. A. R. Chraplyvy, R. W. Tkach, L. L. Buhl, and R. C. Alferness, Electron. Lett. **22**, 409 (1986).
14. F. Devaux, Y. Sorel, and J. F. Kerdiles, IEEE J. Lightwave Technol. **11**, 1937 (1993).
15. G. P. Agrawal, *Nonlinear Fiber Optics*, 5th ed. (Academic, 2012).
16. J. R. M. Osgood, N. C. Panoiu, J. I. Dadap, X. Liu, X. Chen, I.-W. Hsieh, E. Dulkeith, W. M. Green, and Y. A. Vlasov, Adv. Opt. Photon. **1**, 162 (2009).
17. K. Dolgaleva, W. C. Ng, L. Qian, and J. S. Aitchison, Opt. Express **19**, 12440 (2011).
18. M. Dinu, F. Quochi, and H. Garcia, Appl. Phys. Lett. **82**, 2954 (2003).